Ates Erk[1]
Edme H. Hardy[2]
Tim Althaus[3]
Werner Stahl[2]

[1] BASF AG, Ludwigshafen, Germany.
[2] Institut für Mechanische Verfahrenstechnik und Mechanik, Universität Karlsruhe (TH), Germany.
[3] Institut für Lebensmittel- und Ernährungswissenschaften, ETH, Zürich, Switzerland.

Full Paper

Filtration of Colloidal Suspensions – MRI Investigation and Numerical Simulation

The principle mechanisms of solid-liquid separation processes are sedimentation and filtration, both including the formation and compression of a liquid-saturated bulk. The compressive properties of the bulk determine the operating parameters of solid-liquid separation devices and the achievable separation results. Information about the solids volume fraction of the bulk is essential for a better understanding of the physical mechanisms and precise modeling. A numerical model for the calculation of the local solids volume fraction during formation and compression of filter cakes and sediments was developed. The calculated results are compared with experimental NMR data.

Keywords: Colloids, Filtration, Nuclear magnetic resonance (NMR), Simulation, Suspensions

Received: February 3, 2006; *accepted:* March 17, 2006

DOI: 10.1002/ceat.200600054

1 Introduction

Solid-liquid separation of fine particulate suspensions is of importance in many fields of process technology. Examples include the industrial production of pigments and ceramics such as titania, alumina, and kaolin, as well as food processing and wastewater treatment. The principle mechanisms of solid-liquid separation processes are sedimentation and filtration. Both cases include the formation and compression of a liquid-saturated bulk (sediment or filter cake). The compressive properties of the bulk determine the operating parameters of solid-liquid separation devices and the achievable separation results.

The solids volume fraction of the bulk strongly depends on the local stress. In the transient state a liquid transport within the porous system takes place. As a result, a time-dependent gradient of the solids volume fraction develops. Spatially resolved information about the solids volume fraction as a function of time under different conditions (e.g., pressure, pH) allows a better understanding of the physical mechanisms and, thus, more precise modeling. The required data can be gained by magnetic resonance imaging (MRI) in a nondestructive and highly resolved way.

In this paper, experimental and calculated results concerning solids volume fraction profiles during the formation and compression of fine particulate filter cakes are presented. A numerical model for the calculation of the local solids volume fraction during formation and compression of filter cakes and sediments was developed. The calculated results are compared with the experimental NMR data.

This work focuses on the application of a model and a numerical simulation program for describing dynamic filtration processes and its validation by means of in situ NMR measurements. Further, this research is aimed at gaining a better understanding of the structural changes within fine particulate filter cakes during their formation and consolidation and at investigating the influence of interparticle forces.

The description of dynamic filtration and consolidation processes used for this work is based on an approach and a numerical algorithm developed by Bürger et al. [1, 2]. In this model the material properties are characterized by two material functions: the permeability as a function of the solids volume fraction, $k(\phi)$, on the one hand, and the compressive yield stress as a function of the solids volume fraction, $p_s(\phi)$, on the other hand[1)].

The permeability k determines the hydrodynamic interaction between the solid and the liquid phase and, thus, the kinetics of the fluid transport within the filter cake. The compressive yield stress p_s is a measure for the strength of a particle network in compression and determines the equilibrium solids concentration reached at a certain applied pressure. Furthermore, the fluid viscosity and the density difference between the solid and the liquid phase have to be known.

Implementation of the model and the material functions in a numerical simulation program allows the calculation of the local solids volume fraction within a filter cake as a function of

Correspondence: Dipl.-Ing. A. Erk (ates.erk@basf.com), BASF AG, GCT/R-L549, D-67056 Ludwigshafen, Germany.

1) List of symbols at the end of the paper.

operating parameters and time. The required data to specify the filtration process includes the initial solids volume fraction ϕ_0, the initial suspension mass per unit filtration area, the applied pressure difference Δp and the flow resistance of the filter medium. The program code used to calculate the results shown below was implemented in Matlab 6.5 (The Mathworks Inc.).

For the simulation of the filtration process, the solid-liquid-system is divided into several slices parallel to the plane of the filter medium. A typical slice thickness used in this study was 0.1 mm.

The permeability and the compressive yield stress of fine particulate solid-liquid systems strongly depend on particle-particle interactions which can be controlled by adjusting the pH and the ionic strength. To investigate the effect of interparticle forces on filtration kinetics and cake structure, the experimental determination of the material functions as well as NMR measurements were carried out at different pH values.

For characterizing particle-particle interactions the zeta potential ζ was used. According to the DLVO theory, the net interaction between particles at high absolute values of the zeta potential (approx. $\zeta > 40$ mV) is repulsive, at the isoelectric point (iep, $\zeta = 0$) it is attractive [3].

2 Experimental

A fine particulate aqueous alumina suspension was examined (Alcoa, CT 3000 SG, mean particle diameter: 0.6 μm). The water used in this study was ion-exchanged and had a conductivity of less than 2 μS/cm. The pH was adjusted using HCl and NaOH. Zeta potential measurements were conducted with an Acoustosizer II (Colloidal Dynamics).

NMR measurements were carried out with an in situ filtration cell integrated into a NMR tomograph (Bruker Avance 200 SWB) for spin density measurement (^{1}H-NMR), for details, see, e.g., [4].

A detailed view of the filtration cell with an outer diameter of 25 mm is given in Fig. 1. The cell is constructed of nonmetal materials such as PMMA, PVC, and PTFE. As filter medium a membrane with 0.2 μm pore diameter was used (Pall, Germany).

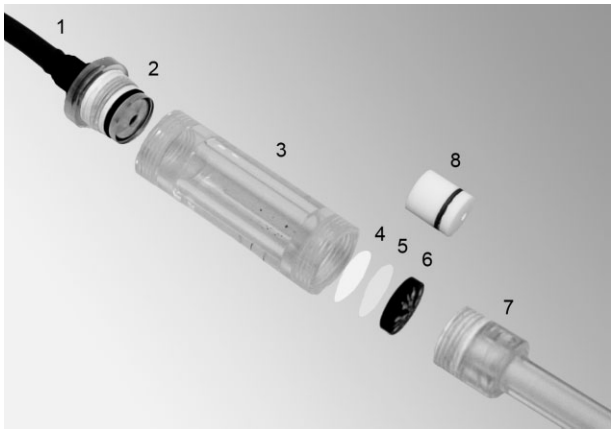

Figure 1. Filter cell for in situ NMR measurements: (1) inlet for pressurized air, (2) lid, (3) filtration ring (PMMA), (4) filter medium, (5) support cloth, (6) perforated support plate (PVC), (7) filtrate outlet, (8) piston (PTFE, optional).

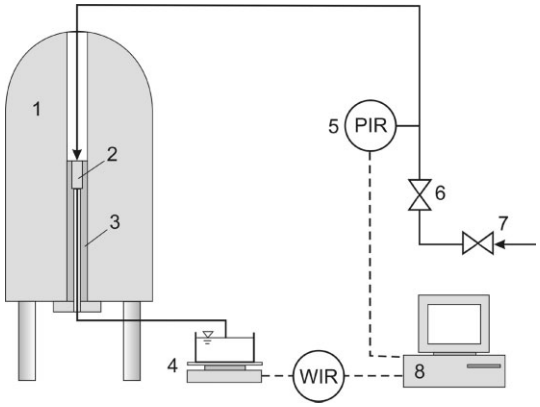

Figure 2. Experimental setup for in situ NMR measurements of filtration processes. (1) NMR Tomograph, (2) filter cell, (3) probe head, (4) balance, (5) digital manometer, (6) pressure valve, (7) air pressure inlet, (8) computer.

Fig. 2 shows a schematic drawing of the complete experimental setup. The pressure difference was adjusted using a valve and a digital manometer. The filtrate was collected on a highly accurate balance. Pressure difference and filtrate mass were registered by a computer as a function of time.

For the spatially resolved determination of the spin density a spin-echo pulse sequence based on a work by Horsfield, Fordham and Hall [5] was used (one-dimensional resolution of 230 μm, absolute measuring time $<< 1$ s). During each filtration process a series of one-dimensional NMR scans was performed until the end of the consolidation of the filter cake was reached.

The NMR signal was correlated with the solids volume fraction in the probe by means of a calibration curve generated by measuring the NMR signal of probes with known solids volume fraction. Inhomogeneities of the magnetic field were corrected by normalizing the NMR signal with the signal of reference measurements with pure water.

The material functions $k(\phi)$ and $p_s(\phi)$ were determined with a compression-permeability cell (CP cell).

3 Results

3.1 Preliminary Investigations

First, filtration experiments within and outside the NMR tomograph were carried out in order to examine the influence of the magnetic field on the filtration behavior of the alumina suspension. The results showed good agreement, allowing the conclusion that the influence of the magnetic field could be neglected.

The relationship between the NMR signal and the solids volume fraction needed for calibration is shown in Fig. 3.

The experimentally determined material functions applied for the numerical simulation of the filtration processes are pre-

sented in Figs. 4 and 5. Fig. 4 shows the permeability as a function of the solids volume fraction at two different pH values or zeta potentials. At pH 4 the permeability is much lower than at pH 8.6 (see Fig. 10). The dependency of the compressive yield stress on the solids volume fraction and the zeta potential is illustrated in Fig. 5.

Because of the increasing repulsive forces between the particles the network stability decreases with increasing absolute value of the zeta potential. This leads to a shift of the functions $p_s(\phi)$ and $k(\phi)$ towards higher solids volume fractions.

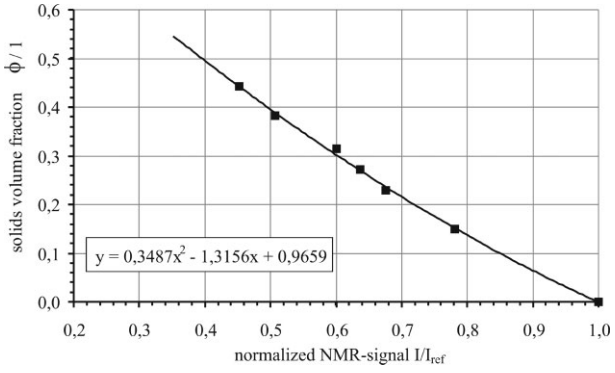

Figure 3. Calibration curve for correlation of solids volume fraction within alumina filter cake and normalized NMR signal.

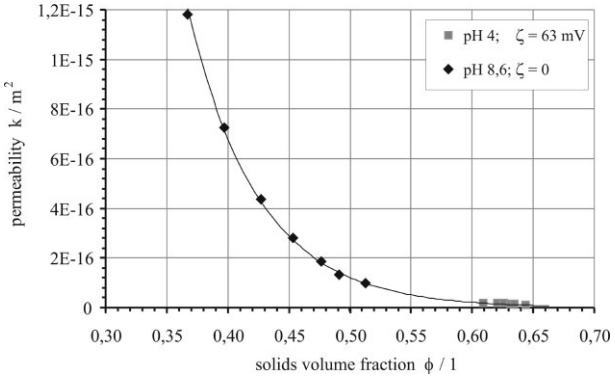

Figure 4. Permeability as a function of solids volume fraction at different zeta potentials (alumina, CP cell measurements).

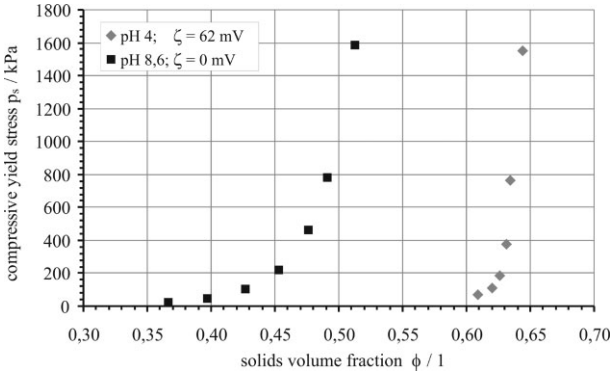

Figure 5. Compressive yield stress as a function of solids volume fraction and zeta potential (alumina, CP cell measurements).

3.2 Comparison between NMR Data and Simulation Results

Fig. 6 shows an experimental result of a filtration process carried out within the NMR tomograph at a pressure difference of 41 kPa, an initial solids volume fraction of 0.095 and a zeta potential of zero (iep, attractive interparticle forces). The solid lines represent lines of constant solids volume fraction. After 1000 s the cake height measures 5 mm and the distance between the surface of the remaining suspension and the surface of the filter cake is approximately 2 mm. The maximum solids volume fraction reached at the bottom of the filter cake is 0.38–0.39. Due to the meniscus at the suspension surface the NMR signal does not drop to zero immediately which causes the presence of several isoconcentration lines in this area (artefact).

The corresponding simulation result is presented in Fig. 7. Obviously, there is good agreement between the calculated and the experimentally determined data. The simulation yields a

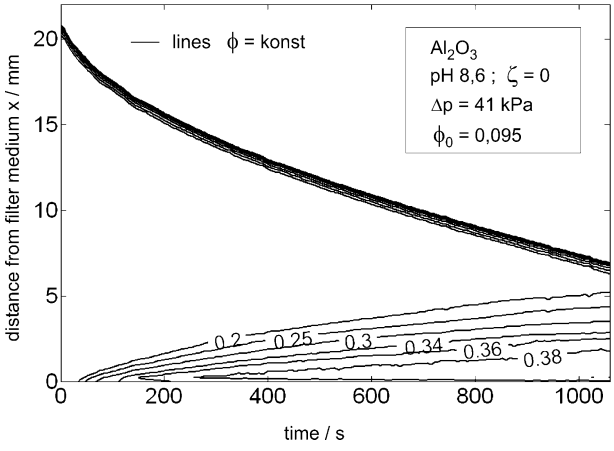

Figure 6. NMR measurement: filtration of an alumina suspension at pH 8.6 (iep).

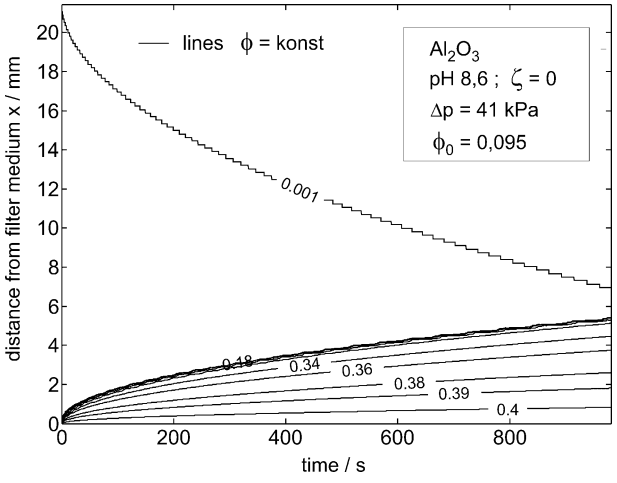

Figure 7. Numerical simulation: filtration of an alumina suspension at pH 8.6 (iep).

cake height of 5.3 mm and a remaining suspension level of 2 mm above the cake after a filtration time of 1000 s. The maximum solids volume fraction reached at the bottom of the filter cake is 0.4.

The results for a zeta potential of 62 mV (highly repulsive interparticle forces) are shown in Figs. 8 and 9. NMR data for the filtration of an alumina suspension at a pressure difference of 111 kPa and an initial solids volume fraction of 0.117 are presented in Fig. 8. After 1200 s the cake height measures less than 2 mm and the distance between the suspension interface and the surface of the filter cake is 15 mm.

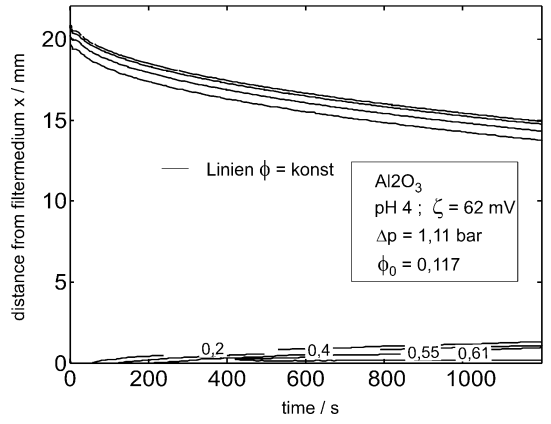

Figure 8. NMR-measurement: filtration of an alumina suspension at pH 4 (ζ = 62 mV).

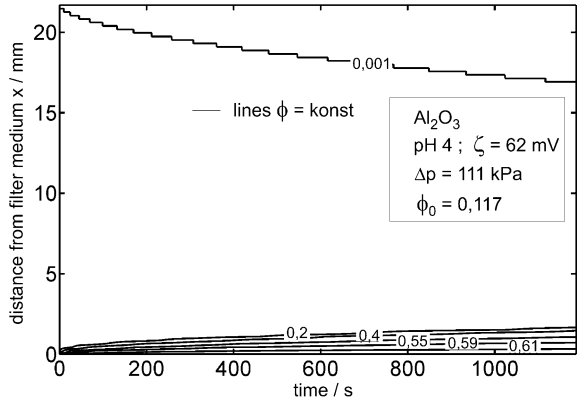

Figure 9. Numerical simulation: filtration of an alumina suspension at pH 4 (ζ = 62 mV).

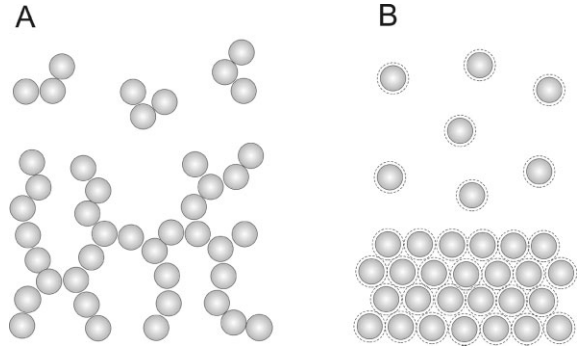

Figure 10. Schematic illustration of filter cake microstructure in the case of attractive (A) and repulsive (B) interparticle interactions.

Fig. 9 shows the simulation data corresponding to the NMR filtration experiment displayed in Fig. 8. Although there are minor differences concerning cake height and suspension level, simulation and experiment are in good agreement. The calculated maximum solids volume fraction reaches the same value as in the experiment.

The extremely slow cake build-up is caused by the low permeabilty of the densely packed cake which shows solids volume fractions of up to 0.61. The thin cake layer acts as a bottleneck for the suspension above.

The high solids volume fraction within the filter cake at ζ = 62 mV is caused by the repulsive interparticle forces, allowing the particles to be arranged in a very close packing (see Fig. 10(B)). If the particle interactions are attractive, a much more porous network with a higher permeability is formed, leading to faster filtration rates (see Fig. 10(A)).

In conclusion, it can be stated that the applied filtration model combined with the experimentally determined material functions is able to describe the filtration of the investigated alumina suspension in an accurate way. The strong effects of variable interparticle forces on the cake structure and filtration kinetics were well captured both by NMR measurements and numerical simulation.

Acknowledgements

Financial support by the DFG (FOR 338) is gratefully acknowledged. The authors would like to thank F. Flügel and E. Oliver-Gonzalez for their technical support.

Symbols used

I/I_{ref}	[–]	normalized NMR signal intensity
k	[m^2]	permeability
p_s	[N/m^2 = Pa]	compressive yield stress
Δp	[N/m^2 = Pa]	applied pressure difference
ϕ	[–]	solids volume fraction
ϕ_0	[–]	initial solids volume fraction
ζ	[mV]	zeta potential

References

[1] R. Bürger, F. Concha, K. H. Karlsen, *Chem. Eng. Sci.* **2001**, *56*, 4537.
[2] R. Bürger, F. Concha, *Int. J. Miner. Process.* **2001**, *63*, 115.
[3] Z. Zhou, P. J. Scales, D. V. Boger, *Chem. Eng. Sci.* **2001**, *56*, 2901.
[4] E. H. Hardy, *Chem. Eng. Technol.* 2006, 29 (7), 785. DOI: 10.1002/ceat200600046
[5] M. A. Horsfield, E. J. Fordham, L. D. Hall, *J. Magn. Reson.* **1989**, *81*, 593.

